

## INDICATIONS OF INTERMEDIATE COMPOSITIONS IN THE BaSO<sub>4</sub>-SrSO<sub>4</sub> SOLID-SOLUTION SERIES FROM THE BAHÇECİKTEPE CELESTINE DEPOSIT, SİVAS, EAST-CENTRAL ANATOLIA, TURKEY

ERDOĞAN TEKİN<sup>§</sup>, BAKİ VAROL AND İ. SÖNMEZ SAYILI

*Department of Geological Engineering, Faculty of Engineering, Ankara University, 06100, Tandoğan – Ankara, Turkey*

YALÇIN ELERMAN

*Department of Physical Engineering, Faculty of Engineering, Ankara University, 06100, Tandoğan – Ankara, Turkey*

### ABSTRACT

Various types of celestine occurrences are hosted by Tertiary evaporite deposits and molasse-type sediments of the Sivas Basin, in east-central Anatolia, Turkey. Celestine mineralization occurs in various sedimentary facies, including clastic, carbonaceous and evaporitic. Mineralization in the Ba-Sr sulfate solid-solution series is found in a few samples from the Bahçeciktepe celestine deposit, one of the typical mineralized sites in the Basin. Samples with a dendritic structure have karstic dissolution-induced voids and usually show a travertine-like texture; some are crystallized in fibroradial and subhedral tabular forms. In addition, clay envelopes around crystals and compositional and sector zoning of the crystals are typical features. XRD, electron-microprobe, single-crystal XRD and AAS analyses of the same samples suggest the presence of intermediate compositions in the BaSO<sub>4</sub>-SrSO<sub>4</sub> solid-solution series, as well as compositions close to the end members.

*Keywords:* barite, celestine, intermediate compositions, (Ba,Sr)SO<sub>4</sub> solid solution, sector zoning, Sivas Basin, Turkey.

### SOMMAIRE

Plusieurs sortes d'indices de célestine sont présentes dans les évaporites tertiaires et les sédiments de type molasse dans le bassin de Sivas, secteur centre-est de l'Anatolie, en Turquie. La minéralisation en célestine est développée dans plus d'un milieu sédimentaire, y inclus clastique, carbonacé et évaporitique. La minéralisation a donné des compositions le long de la solution solide entre BaSO<sub>4</sub> et SrSO<sub>4</sub> dans le gisement de Bahçeciktepe, typique des sites minéralisés dans ce bassin. Des échantillons ayant une forme aciculaire montrent une texture karstique due à la dissolution, et en général une texture semblable à celle du travertin; certains échantillons montrent un habitus fibroradié ou en plaquettes sub-idiomorphes. De plus, une enveloppe d'argiles entoure les cristaux; une zonation en secteur des compositions est courante. Nos analyses en diffraction X, sur poudre ainsi que sur cristal unique, avec une microsonde électronique, et par absorption atomique montrent des indications de la présence de compositions intermédiaires dans la série BaSO<sub>4</sub>-SrSO<sub>4</sub>, ainsi que de compositions proches des pôles.

*Mots-clés:* barite, celestine, compositions intermédiaires, solution solide (Ba,Sr)SO<sub>4</sub>, zonation en secteurs, bassin de Sivas, Turquie.

### INTRODUCTION

The end members of the solid-solution series between celestine and barite are widely distributed. However, intermediate compositions of the series, (Ba,Sr)SO<sub>4</sub>, are subject to ion exchange in response to changes in the composition of the primary solution, after the initial precipitation; as a result, intermediate compositions are rarely found in nature (Burkhard 1978). Puchelt & Müller (1964) found 8.6 mol.% SrSO<sub>4</sub> in the

structure of strontian barite, and attributed such a composition to sedimentary processes within the Zechstein Basin. Malinin & Urusov (1983) synthesized members of the complete solid-solution series by precipitation from a saturated aqueous solution in the range 35°–185°C. Recent studies have shown that crystals in this solid-solution series display compositional zoning, including oscillatory and sector zoning (Putnis *et al.* 1992, Prieto *et al.* 1993, 1997, Hanor 2000).

<sup>§</sup> E-mail address: tekin@eng.ankara.edu.tr

The most important celestine mineralization in Turkey is found in the Tertiary Sivas Basin, in central Turkey, which developed over the Taurus suture zone. Although the celestine mineralization in the basin shows no preference for lithology, it is generally associated with Late Eocene – Miocene evaporitic sequences and occurs at various horizons (Figs. 1a, b). On the basis of their mode of deposition, we have divided these occurrences of celestine in the study area into four categories. These are void-filling, zebra, nodular, and massive celestine deposits. The first type is found in dark brown

turbiditic limestones in the upper parts of the Middle to Late Eocene Bozbel Formation. The second type, the zebra deposits, has bands a few cm to a few meters in thickness, and they are similar to rhythmite of diagenetic origin, as recognized by Amstutz & Fontboté (1982). The third group, nodular celestine, is present in alluvial-fan sediments of the Oligocene Selimiye Formation. Finally, the lenticular deposits of blue massive celestine were formed in massive gypsum of the Middle Miocene Purtepe Member (Gökçe 1990, Tekin *et al.* 1994) (Fig. 2). We focused our investigation on miner-

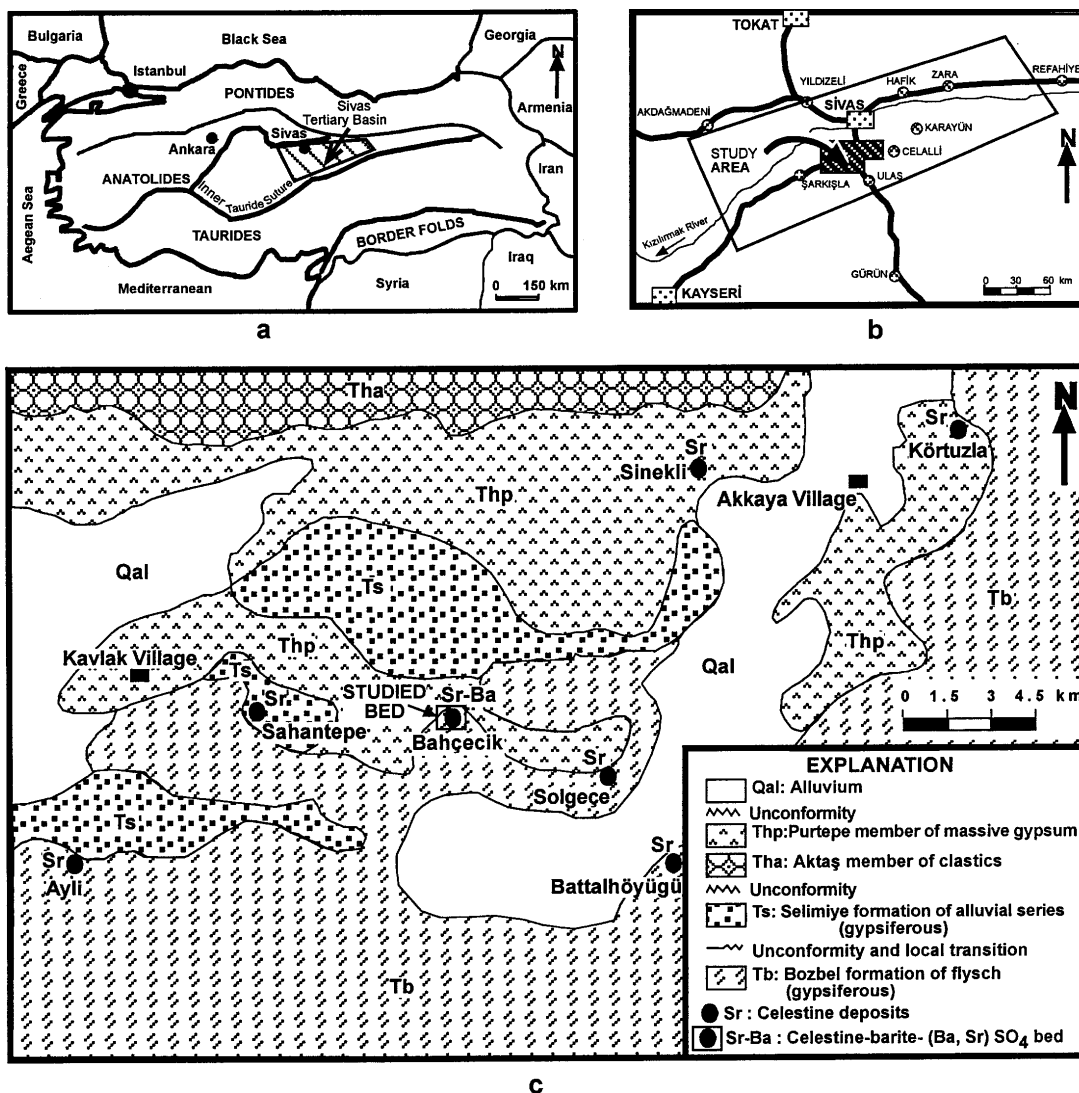


FIG. 1. a) Location of the Tertiary Sivas Basin in Turkey. b) Location map of the study area in the Sivas Basin. c) Simplified geological map of the study area and location of celestine – barite – (Ba,Sr)SO<sub>4</sub> beds.

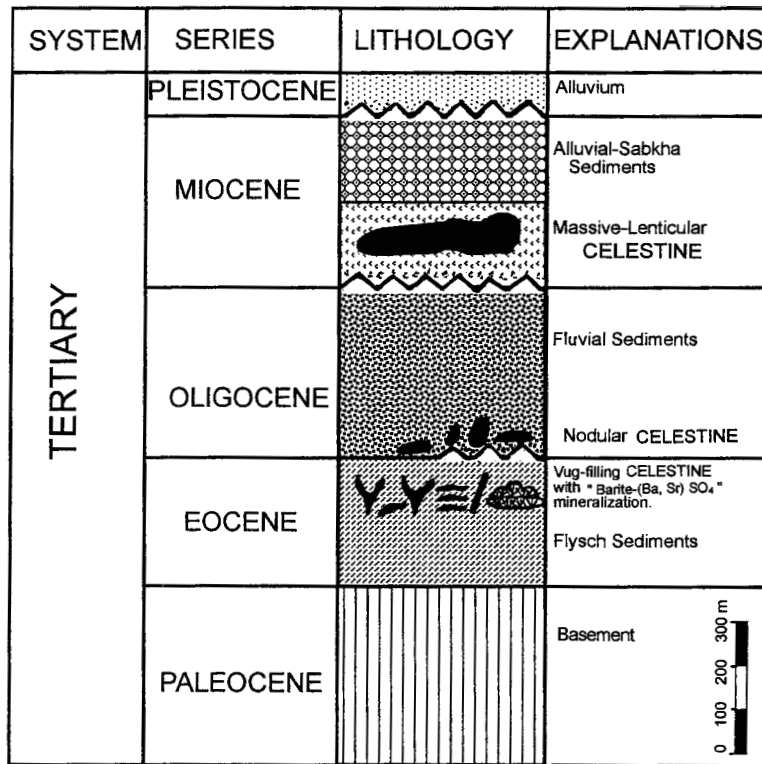


FIG. 2. Simplified Tertiary sequence containing celestine – barite and  $(\text{Ba},\text{Sr})\text{SO}_4$ .

alization at the Bahçeciktepe celestine deposit, one of seven occurrences of celestine identified in the Sivas–Ulaş area of central Anatolia. This deposit is hosted by turbiditic units of the Middle to Late Eocene Bozbel flysch. Celestine mineralization in the Bahçeciktepe deposit generally occurs as fracture fillings and some zebra-type bands having a thickness of 1–3 cm (Tekin 1995). In the lower part of the deposit, there are also local occurrences of some intermediate compositions in the  $(\text{Ba},\text{Sr})\text{SO}_4$  solid-solution series, associated with celestine (Fig. 1c).

The purpose of this study is to document the compositional and sector zoning and to evaluate probable natural intermediate compositions of the  $(\text{Ba},\text{Sr})\text{SO}_4$  solid-solution series by examining the petrographic, microtextural, and geochemical properties of this celestine–barite mineralization in the Bahçeciktepe deposit, compositions that are scarce in nature. In this study, systematic samples from trenches and adits were collected from celestine and barite zones of the Bahçeciktepe celestine deposit, located in the Sivas–Ulaş evaporite basin.

## REGIONAL GEOLOGY

Sedimentary units of Tertiary age in the Sivas–Ulaş region unconformably overlie ophiolites of the Inner Taurus Suture Zone. During the Paleocene–Eocene, reefal limestones were deposited in the marginal parts of the sinking basin while flysch sediments accumulated in the deeper parts. The basin, which took on a regressive character in the Late Eocene, changed to an evaporitic and lagoonal environment. During this phase, gypsum deposition alternated with carbonate and claystone deposition. In the Oligocene, subaerial conditions prevailed in the region, giving rise to fluvial-lacustrine complexes. In the Early to Middle Miocene (?), clastic-reefal carbonate units were deposited during a limited marine transgression. During this period, coastal sabkhas of variable depth formed between topographic highs, and thick, massive gypsum was deposited. Subaerial volcanism also occurred locally in the region. In some cases, this volcanic material extended into playa lakes in the Late Miocene. Pliocene sediments overlie all of these units; they were deposited in a fluvial regime (Fig. 2) (Cater *et al.* 1991, Tekeli *et al.* 1992, Tekin 1995).

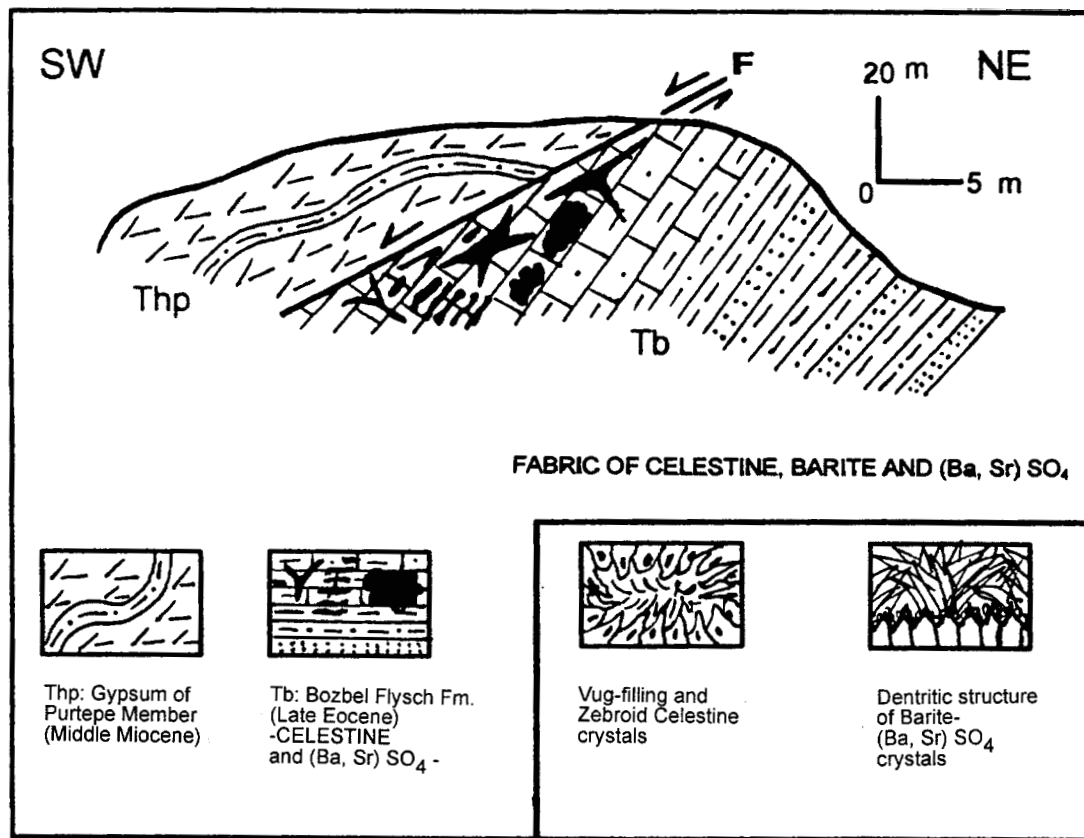


FIG. 3. Schematic portrayal of the position of celestine-barite and (Ba,Sr)SO<sub>4</sub> mineralization in the Bahçeciktepe bed.

#### GEOLOGICAL SETTING OF THE BAHÇECİKTEPE CELESTINE DEPOSIT

The Bahçeciktepe deposit is located 100 m north of Ekincioğlu village. Celestine mineralization occurs in folded, fractured, bioclastic, clayey to sandy limestones of the Middle to Late Eocene Bozbel Formation. The Bahçeciktepe celestine deposit is 30 m wide and 80 m long (Fig. 3). The deposit, as exposed in trenches, comprises celestine as void fillings and of zebra type (Figs. 4a, b). Color changes from yellow to brown in the basement limestones that host the void-filling celestine seem to be indications of hydrothermal alteration (Tekin *et al.* 1994). In addition, Tekin *et al.* (1994) attributed "stalactite"-type occurrences of celestine in this deposit to subsurface karst (thermokarst) formation. According to Tekin (1995), undulating-flow structures and siliceous iron-oxide-rich lenses in the celestine horizons also are signs of hydrothermal activity. Void-filling celestine of

the Bahçeciktepe deposit comprises white, yellow, and orange, pure, prismatic, fibroradial, and fan-shaped crystals in a matrix, with stalactite-like growth into the voids. Prismatic crystals are a few cm in length, whereas those of fibroradial habit are larger, since they grew sequentially (Fig. 4a). Zebra-type celestine mineralization of the Bahçeciktepe deposit comprises medium- to coarse-grained, dirty white, subhedral to euhedral tabular crystals. In addition, small-scale bands of recrystallized calcite, microcrystalline dolomite, organic material, and clay coatings are also observed in the "zebra"-type celestine (Tekin 1995) (Fig. 4b).

The celestine and barite samples investigated were collected from a thin zone along a small fault at the base of the Bahçeciktepe exposure. They have a travertine-like morphology, and are white, dirty white and dark blue. The crystals are acicular, but are partly microcrystalline and massive in the barite-bearing parts of the deposit (Figs. 4c, d).

## PETROGRAPHY

In the Bahçeciktepe deposit, various habits of crystals were recognized in hand samples comprising the white and blue zones. Thin-section studies show that in the white zone, long, thin prismatic tabular crystals give way to fibroradial fan-shaped or rosette-like crystals (Figs. 5a, b). The blue zone comprises fan- and rosette-shaped crystals (Fig. 5c). Fan-shaped crystals were overgrown along a thin (a few mm thick) clayey zone (Fig. 5d).

The prismatic and tabular crystals that make up the white zone are subhedral and have a relatively high relief. In addition, they have two cleavages, one well developed and one poorly developed (Figs. 5a, b). Interference colors are grey-yellow of the first order; the crystals show a parallel extinction. The sign of elongation is positive. The indices of refraction are  $n_x$  1.594,  $n_y$  1.592, and  $n_z$  1.601 ( $\pm 0.008$ ). Values of the angle  $2V_z$  were measured on 13 crystals using a universal stage and found to average  $49^\circ$ . On the basis of these data, these crystals were determined to be celestine (Fleischer *et al.* 1984).

The fibroradial, fan-shaped or rosette-like crystals are subhedral and have a distinctive relief. They have one well-developed and one poorly developed cleavage (Figs. 5c, d), and show parallel extinction. Their interference colors are grey and yellow-orange of the first order. The sign of elongation is positive. The indices of refraction are  $n_x$  1.616,  $n_y$  1.611, and  $n_z$  1.623 ( $\pm 0.006$ ). The average value of the angle  $2V_z$ , measured on nine grains (crystals), is  $39^\circ$ . Considering all of these data, we infer that the grains in question are barite (Tröger 1971).

MICROTTEXTURAL CHARACTERISTICS:  
RESULTS OF SEM STUDIES

We have documented by SEM studies the microtextural characteristics of barite, celestine and intermediate compositions of  $(\text{Ba}, \text{Sr})\text{SO}_4$  (Appendix 1 presents details of the analytical techniques used in this investi-

gation). The edges of crystals in celestine-bearing zones (A and B<sub>1</sub>) have rod-like prismatic shapes with growth structures as shown in Figure 6a. During karst formation, this type of crystal in places fills pores, growing in a stalactite-like fashion (Fig. 6b). Barite-bearing zones display a tabular morphology of partly fibrous and subhedral shapes. No etching or dissolution textures developed in these zones (Fig. 6c). In horizontal sections taken along their "c" axes, these crystals have a layered sequence and a partly lobate structure. In addition, a 10  $\mu\text{m}$ -thick clayey band was detected between barite and the  $(\text{Ba}, \text{Sr})\text{SO}_4$  intermediate compositions (Fig. 6d). This thin clayey band probably indicates the locus of flow of hot solutions at different phases of subsurface formation of karst during the precipitation of the intermediate compositions of the solid-solution series (Tufar 1979).

EDS studies carried out on these three zones reveal the presence of high amounts of Sr, Ba and S, and lesser amounts of Al, Si, Ca, Cu and Zn. Homogenization temperatures and salinity values measured in fluid-inclusion studies of the ore-mineral paragenesis (Tekin *et al.* 1994) support the contention that such trace-element concentrations were present in the hot solutions during the formation of the clayey bands.

## XRD STUDIES

In order to determine the mineralogical composition of the samples evaluated in our petrographic studies, whole-rock powders were analyzed first by XRD. We observed that in diffractograms, the strongest peaks of pure barite and celestine overlap. We included whole-rock powder-diffraction analyses of three macroscopically distinct zones, on the basis of color and textural differences (*i.e.*, A, B<sub>1</sub> and C, Table 1). We determined that the unit-cell parameters of the cream-colored A zone are very similar to values of standard  $\text{SrSO}_4$ . The B<sub>1</sub> zone, comprising samples very near the A zone (Fig. 7), is characterized by unit-cell parameters comparable to those of  $\text{Ba}_{0.5}\text{Sr}_{0.5}\text{SO}_4$ . Many weak satellite reflections of other phases are also present in these zones, but they were ignored. However, C-zone samples have the unit-cell parameters of standard  $\text{BaSO}_4$  (Table 1).

On the basis of the data obtained from whole-rock powder-diffraction analyses, single-crystal XRD studies were carried out to determine the unit-cell parameters of crystals in the A and B<sub>1</sub> zones. An orthorhombic cell and the unit-cell parameters  $a$  7.048(3),  $b$  8.568(3),  $c$  5.419(2) Å were determined from short-period  $a$ -axis oscillation and long-period  $hk0$ -layer Weissenberg photographs. X-ray-diffractometer analyses were done on a single rod-shaped crystal from the uppermost part of the A zone. These values are consistent with the  $a$ ,  $b$  and  $c$  cell parameters of barian celestine  $(\text{Ba}_{0.5}\text{Sr}_{0.5})\text{SO}_4$  (Goldish 1989). As the B<sub>2</sub> and C (blue, massive) zones are microcrystalline, no single crystal could be obtained, and the cell parameters could not be determined.

TABLE 1. UNIT-CELL PARAMETERS FOR  
BARIUM-STRONTIUM SULFATES

Compositions	Zone	$a$ (Å)	$b$ (Å)	$c$ (Å)	References
$\text{BaSO}_4$	-	7.156(3)	8.881(4)	5.454(2)	ASTM (1972)
$(\text{Ba}_{0.5}\text{Sr}_{0.5})\text{SO}_4$	-	7.006(2)	8.604(4)	5.421(2)	Goldish (1989)
$\text{SrSO}_4$	-	6.866(2)	8.359(3)	5.352(2)	Swanson & Fuyat (1953)
$\text{BaSO}_4$	C	7.159(3)	8.877(4)	5.452(2)	This work
$(\text{Ba}_{0.5}\text{Sr}_{0.5})\text{SO}_4$	B <sub>1</sub>	7.048(3)	8.568(3)	5.419(2)	This work
$\text{SrSO}_4$	A	6.869(2)	8.364(3)	5.345(3)	This work

ASTM (1972): Inorganic index to the powder diffraction file. Joint Committee on Powder Diffraction Standards, PDF 24-1035. The original values on this card (Swanson *et al.* 1972) are:  $a$  7.1563(3),  $b$  8.8811(4),  $c$  5.4541(3) Å,  $\lambda = 1.54051$  Å.

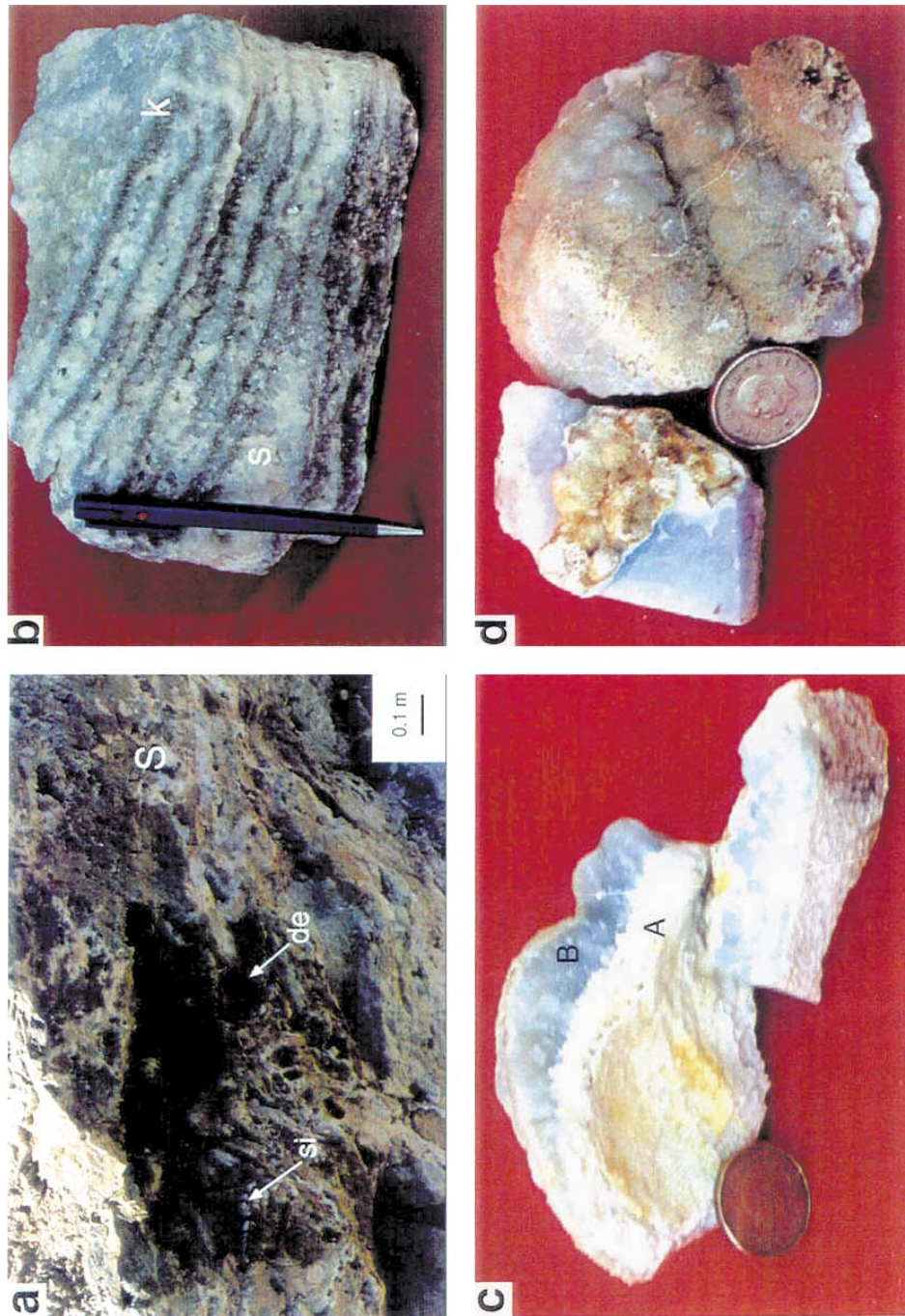


FIG. 4. a) Vug- and void-filling celestine mineralization in clayey-sandy limestones of the Bahçeciktepe celestine deposit, Late Eocene Bozbel Formation (Tb in Fig. 3). Hydrothermal alteration, karstic voids and microgeode-like structures in these limestones are typical. Symbols: de: iron-rich lens, si: silica nodule, s: celestine. b) "Zebra"-type occurrence of celestine in the Bahçeciktepe deposit, Bozbel Formation (Tb). Symbols: k: microcrystalline carbonate band, s: tabular band of crystalline celestine. c) Close-up view of the  $(\text{Ba,Sr})\text{SO}_4$  solid-solution sample investigated, characterized by an acicular structure. d) Close-up view of the travertine-like texture (C zone) on the upper surface of the  $(\text{Ba,Sr})\text{SO}_4$  solid-solution sample investigated.

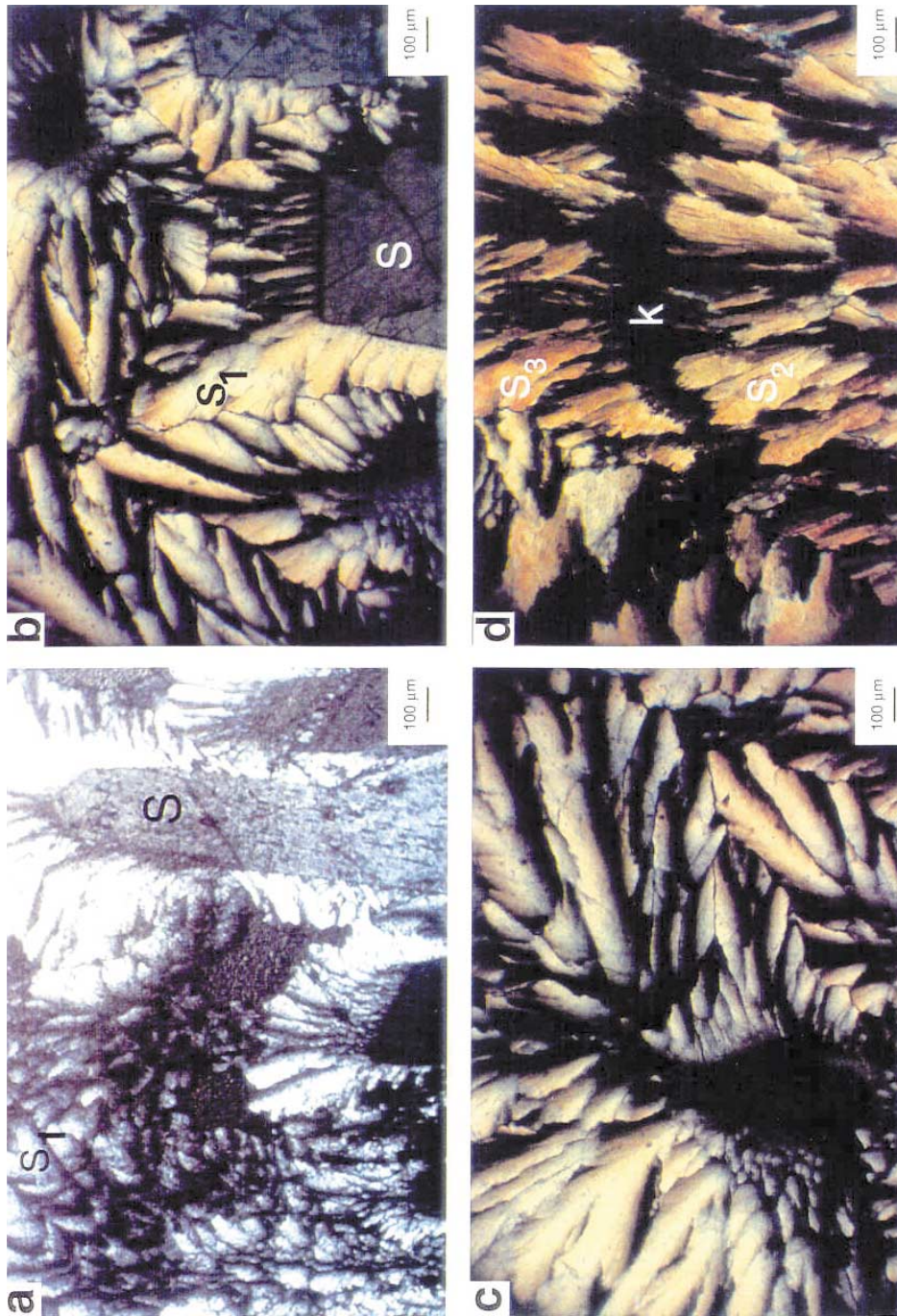


FIG. 5. a) Transition between rod-like crystals of celestine and the crystals with an acicular structure ( $S_1$ ) in the white (A) zone. b) Cross-nicol view of transition between rod-like and fibrous crystals of celestine (S) and acicular ( $S_1$ ) crystals in the white-beige (A) zone. Growth in different directions is typical. c) Cross-nicol view of acicular crystals developed as radial fans. d) Clay-rich band developed in the transition between B and C zones. Symbols: k: clay-rich band,  $S_2$ : acicular crystals of the B zone,  $S_3$ : acicular crystals of the C zone.

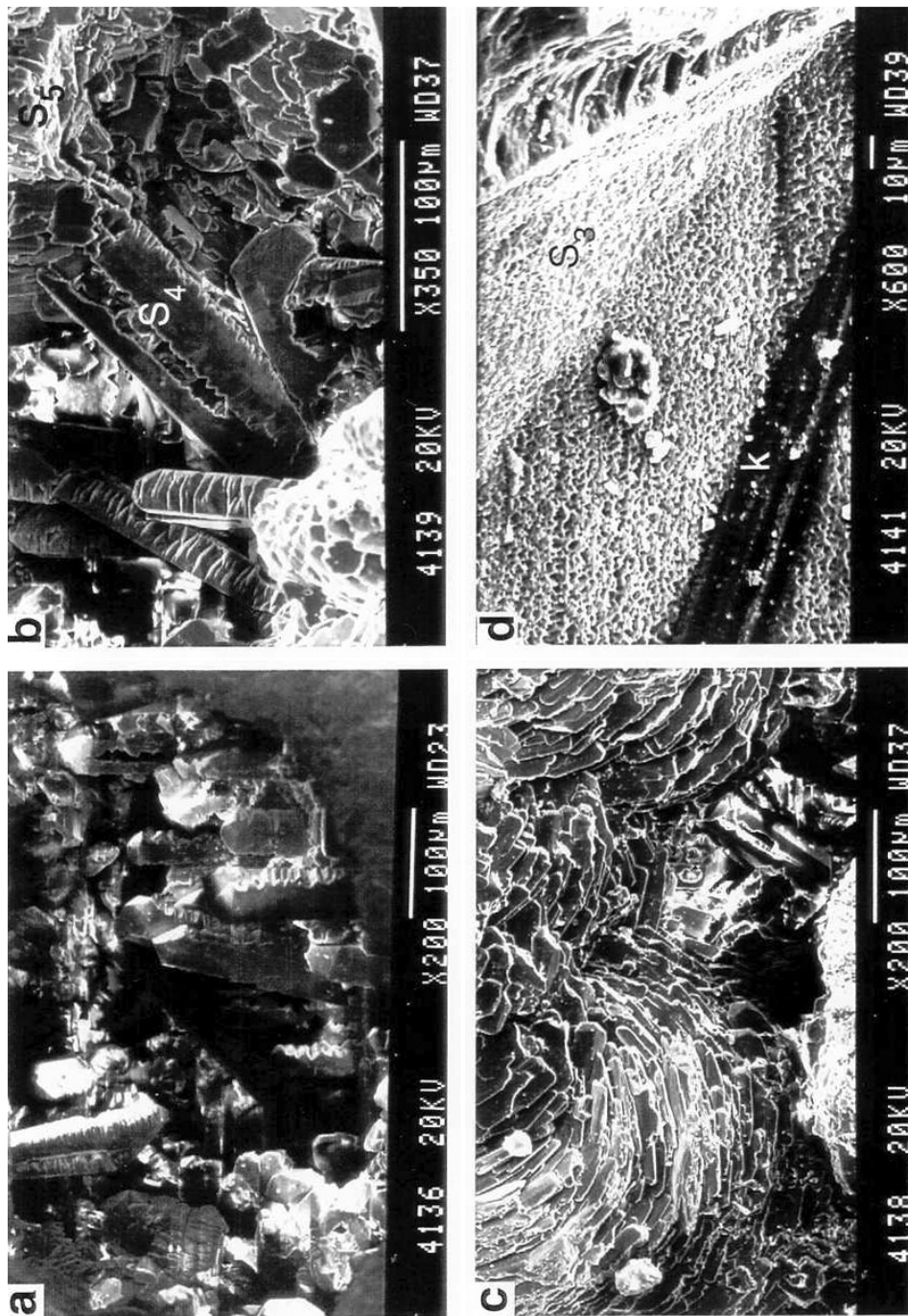


FIG. 6. a) SEM image of rod-like (Ba,Sr)SO<sub>4</sub> crystals (A zone) showing stalactite-like development and zonal growth. b) SEM image of rod-like crystals of (Ba,Sr)SO<sub>4</sub> and subhedral to euhedral, tabular crystals of (Ba,Sr)SO<sub>4</sub> (S<sub>4</sub>). c) SEM image of subhedral to euhedral, tabular crystals of (Ba,Sr)SO<sub>4</sub> in the B and C zones. d) SEM image of clay-rich band observed in the transition between the B and C zones. Travertine-textured crystals (S<sub>3</sub>) above the clay-rich band (k zone) are typical.

## ELECTRON-MICROPROBE (EMP) STUDIES

Electron-microprobe studies were performed to test for the presence of intermediate compositions in the (Ba,Sr)SO<sub>4</sub> solid-solution series. Samples were analyzed from the bottom to the top of the series along traverses at different points. As a result of EMP results, the (Ba,Sr)SO<sub>4</sub> samples were categorized into three main zones. The cream-colored, prismatic-crystalline to acicular A zone comprises the lower part of the sample, representing the bottom of the series. It is followed by the blue, massive B zone, which is, in turn, bounded above by a clayey horizon. The white travertine-like C zone has a fractured or karstic appearance and makes up the upper part of the sample. Acicular crystals in the A zone are nearly pure celestine (Table 2, compositions 1, 2, 3 and 8). The point analyses in the crystals of the transition zone [between the A and B zones in the uppermost part of A zone, toward the B zone (B<sub>1</sub>)] documented compositions around (Ba<sub>0.5</sub>Sr<sub>0.5</sub>)SO<sub>4</sub> (Table 2, compositions 4, 5, 6 and 7). Toward the upper levels in the B zone (B<sub>2</sub>), the point analyses of similar crystals indicate lower Sr and higher Ba contents, with an average composition of (Ba<sub>0.65</sub>Sr<sub>0.35</sub>)SO<sub>4</sub> (Table 2, compositions 9, 10, 11, 12 and 15). Two point analyses from

crystals in the C zone indicate nearly end-member barite (Table 2, compositions 16, 17). Ca contamination (average 1%) of the crystals was also observed in the three zones (Table 2).

During the electron-microprobe analyses, we observed remnants of gypsum and patches of celestine at the margins of the clayey band and in the envelopes of the fractured karstic voids (Fig. 7). A comparison of Ca, Sr and Ba contents reveals a positive correlation between Sr and Ca and a negative correlation between Sr (Ca) and Ba (Table 3). There is no correlation among other major and trace elements. As indicated in Table 2, the Sr/Ba value varies from 112.64 in zone A to 0.06 in zone C. These two values are typical of barite and celestine end-members (Hanor 1968). This trend was also determined in line-scan analyses from zone A (lower zone) to zone C (upper zone) during EDS studies.

## BSE STUDIES

Back-scattered-electron (BSE) imaging analyses were performed on selected samples in order to characterize the compositions of the crystals. Variations in composition lead to variations in image brightness (Lloyd 1987, Shore & Fowler 1996); inhomogeneities and compositional zoning can thus be determined quali-

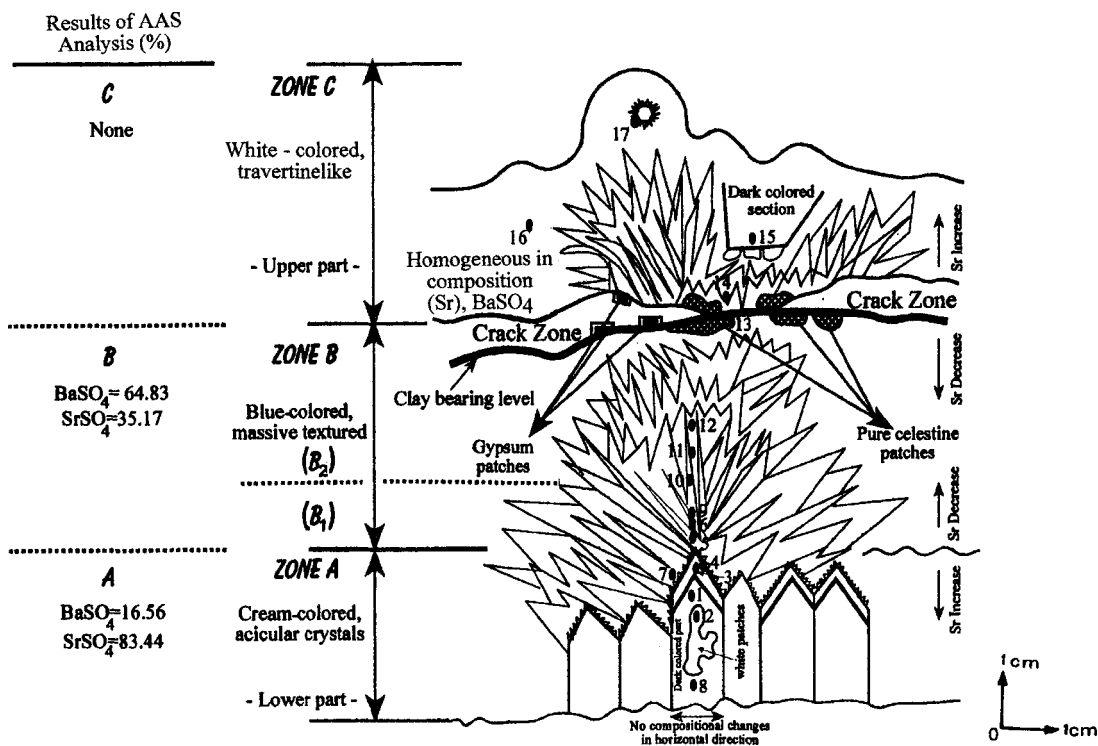


FIG. 7. Schematic appearance of the sample investigated *via* electron-microprobe studies.

tatively. Line profiles show the distribution of substituent ions in the specimens.

A prismatic, acicular crystal representative of zone A was selected for study (Fig. 8a). Whereas celestine is dark, barite or barium-rich parts of these crystals are white (or lighter). It is clear from Figure 8a that barium-rich sectors or patches are present within the celestine. SrSO<sub>4</sub> compositional variations can be detected along the profile, shown as a black line in Figure 8a. The SrSO<sub>4</sub> content varies along the line between 0.8 and 0.4, consistent with sector zoning in the crystal. In Figure 8b, a similar profile for a part of a crystal from zone B<sub>1</sub> is given.

#### ATOMIC ABSORPTION SPECTRA

Chemical analyses from the A and B zones were performed by atomic absorption spectroscopy. Special solutions were prepared from the macroscopically differentiated A and B zones and were analyzed by the flame technique. As a result, BaSO<sub>4</sub> and SrSO<sub>4</sub> concentrations of the A zone were found to be 16.56% and 83.44%, respectively, whereas those of the B zone were found to be 64.83% and 35.17%, respectively (Fig. 7, Table 2). These results indicate that the A zone is richer in Sr; passing through the B zone, the Ba content increases at the expense of Sr.

#### DISCUSSION AND CONCLUSION

The barite and celestine mineralization seems to occur in various environments, ranging from sedimentary (evaporitic and non-evaporitic) to non-sedimentary (epigenetic and hydrothermal) conditions (Brodtkorb 1989). Scholle *et al.* (1990) pioneered studies of the

sedimentary origin of celestine mineralization in the Karstrygen Formation, central East Greenland. An epigenetic origin is indicated in the studies of Brodtkorb *et al.* (1982) and Kushnir (1986). Intermediate compositions in the Ba–Sr sulfate solid-solution series have only rarely been observed in nature (Brower 1973). Before our work, the supply of Ba<sup>2+</sup>, Sr<sup>2+</sup>, and SO<sub>4</sub><sup>2-</sup> ions necessary for the formation of disordered intermediate compositions in this solid-solution series was believed to be hindered by the formation of strain as a result of substitution. Therefore, intermediate compositions were always studied in the laboratory (Graham 1920, Gordon *et al.* 1954, Starke 1964, Boström *et al.* 1967, Hanor 1968, 1973, Brower & Renault 1971, Brower 1973, Malinin & Urusov 1983, Prieto *et al.* 1993, 1997). The early experimental studies showed that barium is concentrated in the solid phase, whereas strontium is concentrated in the aqueous phase during the slow precipitation of (Ba,Sr)SO<sub>4</sub>. The extremely low solubility of BaSO<sub>4</sub> compared to SrSO<sub>4</sub> (Hanor 2000) suggests that initial crystallization should consist of nuclei somewhat rich in BaSO<sub>4</sub> relative to the aqueous phase. Based on diagrams of X(BaSO<sub>4</sub>) versus X(SrSO<sub>4</sub>) (Glynn & Reardon 1990, Prieto *et al.* 1997), only a very small range of aqueous-phase compositions can coexist in equilibrium with solid solutions in the range 0.1 < X(SrSO<sub>4</sub>) < 0.9 (Prieto *et al.* 1993). Some investigators have attributed this result to the differential solubilities of the barite and celestine end-members. Gordon *et al.* (1954) analyzed aqueous solutions during the precipitation of barite and celestine, and determined that Sr had a heterogeneous distribution all along the solid-solution series. Hanor (1968) also reported that depending on changes in solution composition, intermediate (Ba,Sr)SO<sub>4</sub> compositions cannot re-equilibrate and, as a result, intermediate compositions between barite and celestine cannot form. But recent studies performed with reactants of BaCl<sub>2</sub>, SrCl<sub>2</sub> in a solution reservoir and Na<sub>2</sub>SO<sub>4</sub> in another reservoir connected through a column of porous silica hydrogel at 25 ± 0.1°C (Prieto *et al.* 1993,

TABLE 2. RESULTS OF ELECTRON-MICROPROBE ANALYSES, (Ba,Sr)SO<sub>4</sub> FROM THE BAHÇECİKTEPE DEPOSIT, CENTRAL ANATOLIA, TURKEY

Zone	Point Nr.	SrSO <sub>4</sub> %	BaSO <sub>4</sub> %	CaO %	(CaSO <sub>4</sub> ·2H <sub>2</sub> O) %	SrSO <sub>4</sub> /BaSO <sub>4</sub>	Results of AAS analysis %
Zone C	17	5.27	88.00	0.15	(0.46)	0.06	Not analyzed
	16	5.20	73.66	1.04	(3.19)*	0.07	
	15	24.32	69.39	0.00	-	0.35	
Zone B	14	4.07	90.91	0.27	(0.83)	0.04	35.17% SrSO <sub>4</sub> , 64.83% BaSO <sub>4</sub>
	13	5.93	86.75	0.00	-	0.07	
	12	22.16	71.88	0.00	-	0.31	
	11	20.04	74.54	0.10	(0.31)	0.27	
	10	30.71	65.36	0.14	(0.43)	0.47	
	9	34.35	61.56	0.00	-	0.55	
	8	99.98	0.00	0.43	(1.32)	0.00	
Zone A	7	44.09	53.38	0.00	-	0.83	83.44% SrSO <sub>4</sub> , 16.56% BaSO <sub>4</sub>
	6	49.89	48.82	0.00	-	1.02	
	5	51.22	47.56	0.20	(0.61)	1.08	
	4	62.34	33.94	0.00	-	1.84	
	3	92.96	6.87	0.00	-	13.53	
	2	91.10	7.10	0.00	-	12.83	
	1	95.74	0.85	0.31	(0.95)	112.64	

Zone C: white, travertine-like, upper part. Zone B: blue, massive. Zone A: cream-colored, acicular crystals, lower part. \* 13.03% SiO<sub>2</sub>.

TABLE 3. TABLE OF CORRELATIONS OF ELECTRON-MICROPROBE DATA, (Ba,Sr)SO<sub>4</sub> FROM THE BAHÇECİKTEPE DEPOSIT, CENTRAL ANATOLIA, TURKEY

Zone	color	point number	BaSO <sub>4</sub> %	SrSO <sub>4</sub> %	CaSO <sub>4</sub> ·2H <sub>2</sub> O %
Zone C	white	17	88.00	5.27	0.46
		16	73.66	5.20	3.19
		14	90.91	4.07	0.83
Zone B	blue	11	74.54	20.04	0.31
		10	65.36	30.71	0.43
Zone A	cream	5	47.56	51.22	0.61
		1	0.85	95.74	0.95
		8	0.00	99.99	1.32
Upward trend			increasing	decreasing	decreasing

Result: 1) positive correlation between CaO and SrSO<sub>4</sub>, 2) negative correlation between CaO and BaSO<sub>4</sub>, and 3) other elements exhibit no correlation.

1997) showed that there is a strong preferential partitioning of Ba and Sr, and that only a narrow range of aqueous-phase compositions can coexist in equilibrium with intermediate solid-solutions. At high supersaturations, the range of aqueous solutions from which intermediate solid-solutions can nucleate expands, but the bimodal effect remains (Prieto *et al.* 1997). On the other

hand, as Glynn *et al.* (1990) pointed out, if crystallization occurs in a stirred aqueous solution with a small ratio of precipitated solid to fluid, the composition of the aqueous solution does not vary significantly during the growth process, so that the compositions of the crystals tends to be homogeneous.

Most experiments on the  $(\text{Ba,Sr})\text{SO}_4$  solid-solution series have been conducted on solutions near 25°C. Hot aqueous solutions, especially if they are stirred, can give different results. Such an example is mentioned in the study of Brower (1973) and Hanor (1968).

Dendritic, travertine-like karstic dissolution of void-bearing barite and celestine mineralization in the Bağçekiktepe celestine deposit of the Sivas–Ulaş region is believed to have formed from hot solutions during the epithermal phase. Temperatures were probably between 35° and 185°C, as determined from fluid-inclusion studies (Hanor 1966). Nearly pure celestine formed during sudden cooling, whereas barite formed during partial heating (Burkhard 1978, Prieto *et al.* 1993, Tekin *et al.* 1994, Hanor 2000).

Consequently, the formation of compositional and sector zoning, and intermediate compositions oscillating between 0.4 and 0.75  $X(\text{SrSO}_4)$ , as BSE analyses indicate, must have developed from hot, aqueous solutions during a phase of the process. Experimental studies under controlled conditions reveal that precipitation of the intermediate compositions can take place at various temperatures, such as 18°, 20°, 80°, 83°, 95° and 185°C, as reported by Goldschmidt (1938), Gordon *et al.* (1954), Starke (1964), Blount (1977) and Putnis *et al.* (1992), respectively. The temperature values show that the crystallization of the intermediate compositions took place between 25° and 185°C. There is a fairly significant difference in ionic radii between  $\text{Ba}^{2+}$  and  $\text{Sr}^{2+}$ , 1.34 versus 1.18 Å, respectively; there is also a complete solid-solution between  $\text{BaSO}_4$  and  $\text{SrSO}_4$  at room temperature, at least metastably, as first established by Graham (1920).

Celestine with a travertine-like texture is scarce in deposits of the Sivas–Ulaş Tertiary basin. In fact, this type of mineralization was only observed as a thin zone in the Bağçekiktepe celestine deposit. Therefore, it would have been difficult for previous field investigators (Gökçe 1990, Çubuk *et al.* 1992, Karamandersi *et al.* 1992) to discover this unusual occurrence. Furthermore, petrographic, mineralogical, and geochemical features of the samples from this travertine-like zone are quite different from those more typical of celestine mineralization of the Sivas–Ulaş basin.

Petrographic studies and XRD, EMP, AAS and BSE analyses have shown that compositional and sector zoning are typical features of our samples. Barite, celestine and  $(\text{Ba,Sr})\text{SO}_4$  samples observed at the base of the Bağçekiktepe celestine deposit are considered to be a naturally developed example of the  $\text{BaSO}_4$ – $\text{SrSO}_4$  solid-solution series. Literature surveys indicate that this type of mineralization has, to date, been obtained only *via*

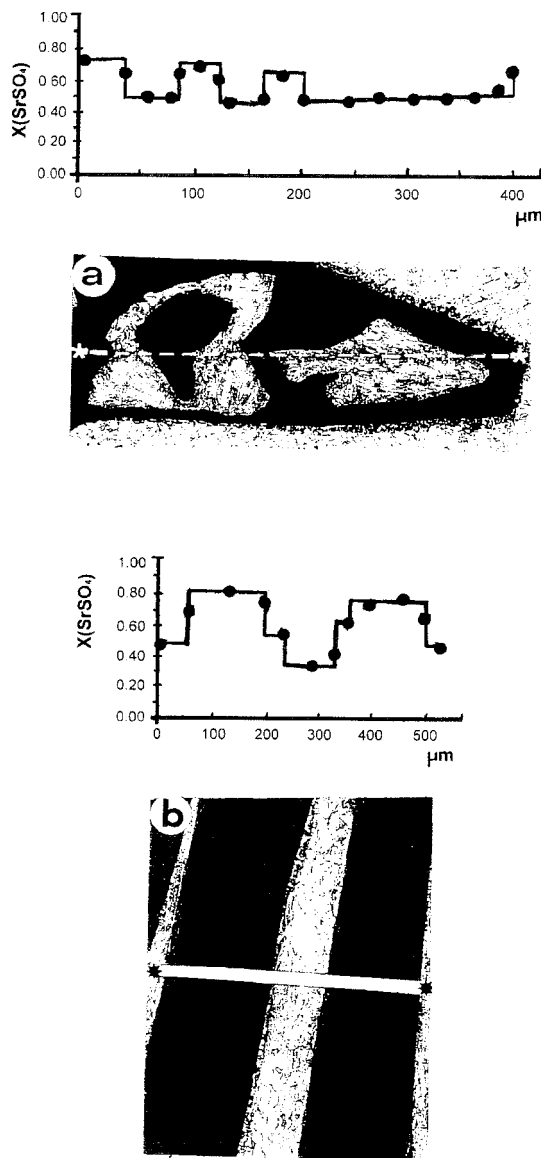


FIG. 8. a) Back-scattered electron images of  $(\text{Ba,Sr})\text{SO}_4$  mixed crystals with oscillatory zoning. b) Back-scattered electron images of  $(\text{Ba,Sr})\text{SO}_4$  crystals with sector zoning.

synthetic methods. Therefore, further studies of the Bahçeciktepe celestine deposit, whose natural (Ba,Sr) SO<sub>4</sub> precipitates seem to be unique, are needed.

#### ACKNOWLEDGEMENTS

The SEM, EMP, XRD, and AAS analyses were carried out in the laboratories of the Turkish Petroleum Corporation (TPAO), General Directorate of Mineral Research and Exploration of Turkey (MTA), Department of Geology, University of Leicester (U.K) and the Research Center of Ankara University, respectively. The authors express their sincere gratitude to the late Dr. A.C. Dunham (University of Leicester, U.K.), Drs. A. Putnis (Münster Universität, Germany), R. Altherr (Heidelberg Universität, Germany) and T. Engin (MTA, Turkey) for critically reviewing an earlier version of the manuscript. Also, the authors thanks to Drs. R.F. Martin (McGill University, Canada) and M.K. Brodtkorb (Servicio Minero Nacional, Argentina) for critically reviewing the last version of the manuscript.

#### REFERENCES

- AMSTUTZ, G.C. & FONTBOTÉ, L. (1982): Observation on the genesis of stratabound Pb–Zn–F–Ba deposits in carbonate rocks. *Proc. Int. Conf. on Mississippi Valley Deposits* (Rolla, Missouri), preprint.
- A.S.T.M. (1972): Inorganic index to the powder diffraction file. Joint Committee on Powder Diffraction Standards.
- BLOUNT, C.W. (1977): Barite solubilities and the thermodynamic quantities up to 300 degrees Celsius and 1400 bars. *Am. Mineral.* **62**, 942-957.
- BURKHARD, A. (1978): Baryt–Celestin und ihre Mischkristalle aus Schweizer Alpen und Jura. *Schweiz. Mineral. Petrogr. Mitt.* **58**, 1-95.
- BOSTRÖM, K., FRAZER, J. & BLANKENBURG, J. (1967): Subsolidus phase relations and lattice constants in the system BaSO<sub>4</sub>–SrSO<sub>4</sub>–PbSO<sub>4</sub>. *Arkiv Mineral. Geol.* **4**, 477-485.
- DE BRODTKORB, M.K. (1989): Celestite: worldwide classical ore fields. In *Nonmetalliferous Stratabound Ore Fields* (M.K. de Brodtkorb, ed.). Van Nostrand, New York, N.Y (17-39).
- \_\_\_\_\_, RAMOS, V., BARBIERI, M. & AMETRANO, S. (1982): The evaporitic celestine, barite deposits of Neuquen, Argentina. *Mineralium Deposita* **17**, 423-436.
- BROWER, E. (1973): Synthesis of barite, celestine and barium–strontium sulfate solid solution crystals. *Geochim. Cosmochim. Acta* **37**, 155-158.
- \_\_\_\_\_ & RENAULT, J. (1971): Solubility and enthalpy of the barium strontium sulfate solid solution series. *New Mexico Bur. Mines, Circ.* **116**.
- CATER, J.M.L., HANNA, S.S., RIES, A.C. & TURNER, R. (1991): Tertiary evolution of the Sivas Basin, central Turkey. *Tectonophys.* **195**, 29-46.
- ÇUBUK, Y., OZANSOY, C. & KAYAN, T. (1992): Geology of Battalhöyüdütepe (Ulaş–Sivas, Turkey) celestine deposits. *Türkiye Jeo. Kurul. Bül.* **7**, 1-7 (in Turkish).
- FLEISCHER, M., WILCOX, R.E. & MATZKO, J.J. (1984): Microscopic determination of the nonopaque minerals. *U.S. Geol. Surv., Bull.* **15**.
- GLYNN, P.D. & REARDON, E.J. (1990): Solid-solution aqueous-solution equilibria thermodynamic theory and representation. *Am. J. Sci.* **290**, 164-201.
- \_\_\_\_\_, \_\_\_\_\_, PLUMMER, L.N. & BUSENBERG, E. (1990): Reaction paths and equilibrium end-points in solid solution aqueous-solution systems. *Geochim. Cosmochim. Acta* **54**, 267-282.
- GOLDISH, E. (1989): X-ray diffraction analysis of barium–strontium sulfate (barite–celestine) solid solutions. *Powder Diffraction* **4**, 214-216.
- GOLDSCHMIDT, B. (1938) : Sur la precipitation mixte des sulfates de barium et de strontium. *C.R. Acad. Sci. Paris* **206**, 1110.
- GORDON, L., REINER, C.C. & BURTT, B.P. (1954): Distribution of strontium with barium sulfate precipitated from homogeneous solution. *Anal. Chem.* **26**, 842-846.
- GÖKÇE, A. (1990): Geology and formation of celestine deposits of south of Sivas. *Cumhuriyet Univ. Müh. Fak. dergi., seri A-yerbilimleri* **6-7**(1-2), 11-27 (in Turkish).
- GRAHMAN, W. (1920): Über Barytocölestin und der Verhältnis von Anhydrit der Cölestin und Baryt. *Neues Jahrb. Mineral.* **1**, 1-23.
- HANOR, J.S. (1966): *The Origin of Barite*. Ph.D. thesis, Harvard University, Cambridge, Massachusetts.
- \_\_\_\_\_ (1968): Frequency distribution of compositions in the barite–celestine series. *Am. Mineral.* **53**, 1215-1222.
- \_\_\_\_\_ (1973): The synthesis of barite, celestite and barium–strontium sulfate solid solution crystal: critical comment. *Geochim. Cosmochim. Acta* **37**, 2685-2687.
- \_\_\_\_\_ (2000): Barite–celestine geochemistry and environments of formation. In *Sulfate Minerals – Crystallography, Geochemistry, and Environmental Significance* (C.N. Alpers, J.L. Jambor & D.K. Nordstrom, eds.). *Rev. Mineral. Geochem.* **40**, 193-275.
- KARAMANDERESI, I.H., KILIÇDAĞI, R. & KILIÇ, N. (1992): Relationship between Sýcakçermik (Sivas) geothermal system and celestine formation. *45. Türkiye Jeo. Kurult. Bildi. Özleri.* **65** (in Turkish).
- KUSHNIR, S.V. (1986): The epigenetic celestine formation mechanism for rocks containing CaSO<sub>4</sub>. *Geochem Int.* **23**, 1-9.

- LLOYD, G.E. (1987): Atomic number and crystallographic contrast images with the SEM: a review of backscattered electron techniques. *Mineral. Mag.* **51**, 3-19.
- MALININ, S.D. & URUSOV, V.S. (1983): The experimental and theoretical data on isomorphism in the (Ba,Sr)SO<sub>4</sub> system in relation to barite formation. *Geokhimiya* **9**, 1324-1334 (in Russ.).
- PRIETO, M., FERNANDEZ-GONZALEZ, A., PUTNIS, A. & FERNANDEZ-DIAZ, L. (1997): Nucleation, growth, and zoning phenomena in crystallizing (Ba,Sr)CO<sub>3</sub>, Ba(SO<sub>4</sub>,CrO<sub>4</sub>), (Ba,Sr)SO<sub>4</sub>, and (Cd,Ca)CO<sub>3</sub> solid solutions from aqueous solutions. *Geochim. Cosmochim. Acta* **61**, 3383-3397.
- \_\_\_\_\_, PUTNIS, A. & FERNANDEZ-DIAZ, L. (1993): Crystallization of solid solutions from aqueous solutions in a porous medium: zoning in (Ba,Sr)SO<sub>4</sub>. *Geol. Mag.* **130**, 289-299.
- PUCHELT, H. & MÜLLER, G. (1964): Mineralogisch-geochemische Untersuchungen an Coelestobaryt mit sedimentären Gefüge. In *Sedimentology and Ore Genesis* (G.C. Amstutz, ed.). Elsevier, New York (143-146).
- PUTNIS, A., FERNANDEZ-DIAZ, L. & PRIETO, M. (1992): Experimentally produced oscillatory zoning in the (Ba,Sr)SO<sub>4</sub> solid solution. *Nature* **358**, 743-745.
- SCHOLLE, P.A., STEMMERIK, L. & HARPOTH, O. (1990): Origin of major karst-associated celestine mineralization in Karstrygen, central East Greenland. *J. Sed. Petrol.* **60**, 397-410.
- SHORE, M. & FOWLER, A.D. (1996): Oscillatory zoning in minerals: a common phenomenon. *Can. Mineral.* **33**, 1111-1126.
- STARKE, R. (1964): Die Strontiumgehalte der Baryte. *Freiberger Forschungs.* **150**.
- SWANSON, H.E., MCMURDIE, H.F., MORRIS, M.C., EVANS, E.H., PARETZKIN, B. & DE GROOT, J.H. (1972): Standard X-ray diffraction powder patterns. *Nat. Bur. Standards, Monogr.* **25**(10), 12-13.
- TEKELI, O., VAROL, B., KESGIN, Y., GÖKTEN, E. & IŞIK, V. (1992): Geology of western of Sivas Basin between Tuzla Lake and Tecer Mountain. *TPAO Co. Report* **3173** (in Turkish).
- TEKIN, E. (1995): *Origin, Sedimentologic and Petrographic Characteristics of Celestine Mineralizations of Sivas Tertiary Basin (Ulaş NW, Turkey)*. Ph.D. thesis, Univ. of Ankara, Ankara, Turkey (in Turkish).
- \_\_\_\_\_, AYAN, Z. & VAROL, B. (1994): Microtextural features and fluid inclusion studies on celestine mineralizations (Sivas-Ulaş, Turkey). *Türkiye Jeo. Bült.* **37**(1), 61-76 (in Turkish).
- TRÖGER, W.E. (1971): *Optische Bestimmung der gesteinsbildenden Minerale* 2 (second ed.). E. Schweizerbart'sche Verlagsbuchhanlung, Stuttgart, Germany.
- TUFAR, W. (1979): Die Lagerstätten Meggen und Dreislar im Sauerland. *Exkursions-führer Deutsch. Geol. Ges.* **A4**, 1-41.

Received April 22, 2001, revised manuscript accepted April 15, 2002.

**APPENDIX 1. MATERIALS AND METHODS**

The samples were studied petrographically in order to select grains for scanning electron microscopy (SEM) with JEOL JSM-840 A and Philips 540-A instruments and energy-dispersion spectroscopy (EDS) with a Tracor TN-5502 instrument in the laboratories of the Turkish Petroleum Corporation (TPAO). The mineralogical composition of samples described in polarizing and electron microscope studies was determined by X-ray diffractometry (Rigaku D-Max 2000 powder diffractometer) in the Central Laboratories for Research and Application of Science and Technology of Ankara University (BITAUM). The X-ray powder-diffraction patterns were produced using  $\text{CuK}\alpha_1$  radiation and a graphite monochromator; calibration was done with silicon. The samples were packed into glass holders, step size was  $0.01^\circ 2\theta$ , and count times were usually 0.3 second per point. All powder-diffraction patterns were analyzed using the JADE 3.1 computer program. Quantitative analyses were done, and the unit-cell parameters were refined. To evaluate the composition of single phases and intergrowths in the (Ba,Sr) $\text{SO}_4$  solid-solution series, electron-microprobe analyses were done with a JEOL Superprobe 733 instrument at the University of Leicester, U.K., and at the Paşabahçe Research

Center, İstanbul, Turkey. Back-scattered electron (BSE) image studies were carried out with a JEOL JSM-6400 scanning electron microscope, and EDS analyses were done with a Noran Instrument Series-2, both in the Department of Metallurgical Engineering, Middle East Technical University, Ankara and with a JEOL JSM-848 A scanning electron microscope in the TPAO Laboratories.

In addition, in order to determine the unit-cell parameters, single-crystal XRD studies were performed with the Philips PW-1130 90/96 X-ray diffractometer at Ankara University. Atomic Absorption Spectrometry (AAS) analyses were done on a Hitachi Z-8200 polarized Zeeman instrument using the flame technique, on samples selected by petrographic and mineralogical investigations at BITAUM. Standards supplied by the Wako Pure Chemical Industrial Ltd. Corp. were used in these analyses. Samples to be analyzed by AAS were powdered in an agate mortar; 0.3 g of the -200 mesh sample and 3 g  $\text{NaCO}_3$  were placed in a platinum dish and heated to 950–1000°C. The sinter was dissolved in distilled water. The metal carbonate precipitates were then filtered and dissolved in 5 mL HCl and diluted to suitable ranges of concentrations.